Determination of Residual Fracture Toughness of Post-fire Concrete Using Analytical and Weight Function Method

YU Kequan[1,*], LU Zhoudao, YU jiangtao

[1] Department of civil engineering, Tongji University, Shanghai 200092, China
* Corresponding author: zjzjykq@163.com

Abstract: Determination of double-K fracture parameter using both analytical and weight function method is carried out in present research. In calculating the cohesive fracture toughness, two situations are divided at critical load. Wedge-splitting tests with ten temperatures varying from 20ºC to 600ºC are implemented. The complete load-crack opening displacement curves are obtained from which the initial and critical fracture toughness could be calculated experimentally. The validation of double-K fracture model to the post-fire concrete specimens is proved. Meanwhile the weight function method agrees well with the analytical method.

Keywords: double-K fracture parameter, analytical method, weight function method, post-fire concrete

1. Introduction

It was established that linear elastic fracture mechanics could be only applicable to large-mass concrete structures and could not be applicable to medium and small-scale concrete structures. Since late 1970s, many nonlinear fracture models have been proposed by various groups of researchers to study the behavior of crack propagation in quasi-brittle materials like concrete [1-6].

Experimental results show that the fracture process of concrete structures undergoes three main stages: (i) crack initiation, (ii) stable crack propagation, and (iii) unstable fracture. Accordingly, the double-K fracture criterion initially introduced by Xu and Reinhardt [6] shows the crack initiation, crack propagation and failure during a fracture process until the maximum load is reached. And the two size-independent parameters, initial cracking toughness, K_I^{ini} and unstable fracture toughness, K_I^{un} can be used to study the crack propagation of concrete.

In order to determine the double-K fracture parameters analytically [7, 8] the value of cohesion toughness, K_I^c due to cohesive stress distribution in the fictitious fracture zone is computed using method proposed by Jenq and Shah [9]. In this method, the determination of K_I^c is done using a special numerical technique because of existence of singularity problem at the integral boundary. Under such circumstances, the use of universal form of weight function will provide a closed form expression for determining the value of K_I^c. And it has proven its accuracy in determining the double-K fracture parameter compared to analytical method [10].

The influences of geometrical parameter [11], specimen geometry [12, 13] and size-effect [7, 8, and 14] on fracture toughness were studied by various researchers. It was found that the influence of a_0/D ratio and shape of test specimen are relatively less than the size- effect on the values of fracture parameters.

The influence of temperature on the fracture parameters was also considered by several researchers, but mainly on the fracture energy and material brittleness [15-19], relatively fewer discussion on the fracture toughness [20-21].s Considering there exist many structures subjected to fire or high temperatures, the influence of temperature on the fracture properties needs further studied.

The present paper is aimed at to determine the residual fracture toughness of wedge splitting specimens subjected to high temperatures and prove the validation of double-K fracture model to the post-fire concrete. The wedge-splitting experiments of totally ten temperatures varying from 20ºC to 600ºC and the specimens size 230×200×200 mm with initial-notch depth ratios 0.4 are implemented. Both analytical and weight function methods are used to calculate the residual fracture toughness parameters. Comparison between the two methods and to experimental results is carried out respectively. From the calculated values of double-K fracture parameters using experimental results the nondimensional parameter, brittleness of concrete may be conceived. Hence, the paper is structured to present the following: (i) details of softening traction-separation law of post-fire concrete, (ii) determination of double-K fracture parameters using existing analytical method, (iii) implementation of weight function method, and (v) experimental validation and comparison of results.

2. Softening traction-separation law of post-fire concrete

The softening traction-separation law is a prior to determine the double-K fracture parameters, at room temperature, many expressions have been proposed based on direct tensile tests [22-26]. Based on numerical studies, simplified bilinear expressions for the softening traction-separation law (illustrated in Fig.1) were suggested by Petersson in 1981[22], Hilsdorft and Brameshuber in 1991 [25], and Phillips and Zhang in 1993 [26]. The area under the softening curve was defined as the fracture energy G_F by Hillerborg et al in 1976 [1]. Therefore, one could get the following equation:

$$G_F = \frac{1}{2}(f_t w_s + \sigma_s w_0) \tag{1}$$

As a consequence, a general form of the simplified bilinear expression of the softening traction-separation law is given as follows:

$$\begin{cases} \sigma = f_t - (f_t - \sigma_s) w/w_0 & 0 \le w \le w_s \\ \sigma = \sigma_s (w_0 - w)/(w_0 - w_s) & w_s \le w \le w_0 \\ \sigma = 0 & w \ge w_0 \end{cases} \tag{2}$$

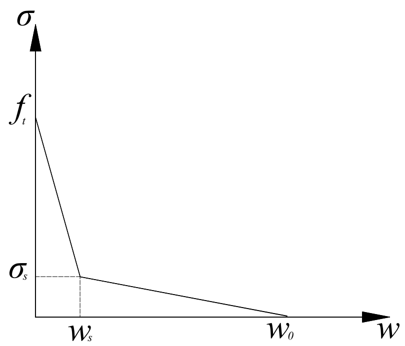

Fig. 1. The bilinear softening traction-separation law

Different values of the break point (σ_s, w_s) and the crack width w_0 at stress-free point were used for the expression proposed by different researchers. In present work, the bilinear softening function of concrete proposed by Petersson is used for post-fire specimens:

$$\begin{cases} \sigma_s = f_t / 3 \\ w_s = 0.8 G_F / f_t \\ w_0 = 3.6 G_F / f_t \end{cases} \tag{3}$$

3. Analytical determination of cohesive fracture toughness

3.1 Effective crack extension length and residual Young's modulus

The linear asymptotic superposition assumption is considered in the analytical method presented by Xu and Reinhardt [7, 8] to introduce the concept of linear elastic fracture mechanics for calculating the double-K fracture parameters. Detailed explanation of the above assumption can be found elsewhere [7].

Based on this assumption, the value of the equivalent-elastic crack length for WS specimen is expressed as:

$$a = (h + h_0)\{1 - (\frac{13.18}{E \cdot b \cdot c + 9.16})^{1/2}\} - h_0 \tag{4}$$

Where $c=CMOD/P$ is the compliance of specimens, b is specimens thickness; h is specimens height and h_0 is the thickness of the clip gauge holder. For calculation of critical value of equivalent-elastic crack length a_c, the value of crack mouth opening displacement ($CMOD$) and P is taken as $CMOD_c$ and P_u respectively.

The residual Young's modulus E is calculated using the P-$CMOD$ curve as:

$$E = \frac{1}{bc_i}[13.18 \times (1-\alpha)^2 - 9.16] \tag{5}$$

Where $c_i=CMOD_{ini}/P_{ini}$, is the initial compliance before cracking, $\alpha= (a_0+h_0)/(h+h_0)$. The value of critical equivalent-elastic crack length a_c and residual Young's modulus E are listed in Table 2.

3.2 Crack opening displacement along the fracture process zone

Since the cohesive stress distribution along the fracture process zone depends on the crack opening displacement and the specified softening law, it is important to know the value of crack opening displacement along the fracture line. It is difficult to measure directly the value of COD along the fracture process zone, for practical purposes the value of $COD(x)$ at the crack length x is computed using the following expression [3]:

$$COD(x) = CMOD\{(1-\frac{x}{a})^2 + (1.018 - 1.149\frac{a}{h})[\frac{x}{a} - (\frac{x}{a})^2]\}^{1/2} \tag{6}$$

For calculation of critical value of crack tip opening displacement $CTOD_c$, the value of x and a (see in Fig.4) in Eq. (6) is taken to be a_o and a_c, respectively. The value of cohesive stress along the fictitious fracture zone to the corresponding crack opening displacement is evaluated using bilinear stress-displacement softening law as given in Eq. 3.

3.3 Determination of stress intensity factor caused by cohesive force

The standard Green's function [27] for the edge cracks with finite width of plate subjected to a pair of normal forces is used to evaluate the value of cohesive toughness. The general expression for the crack extension resistance for complete fracture associated with cohesive stress distribution in the fictitious fracture zone for Mode I fracture is given as below:

$$K_I{}^c = \int_{a_0}^{a} 2\sigma(x)F(\frac{x}{a},\frac{a}{h})/\sqrt{\pi a}\,dx \tag{7}$$

Where

$$F(\frac{x}{a},\frac{a}{h})=\frac{3.52(1-x/a)}{(1-a/h)^{3/2}}-\frac{4.35-5.28x/a}{(1-a/h)}+\left\{\frac{1.30-0.30(x/a)^{3/2}}{\sqrt{1-(x/a)^2}}+0.83-1.76\frac{x}{a}\right\}\left\{1-(1-\frac{x}{a})\frac{a}{h}\right\} \tag{8}$$

and $\sigma(x)$ is the cohesive force at crack length x, see in Fig.3, its expression is shown in Eqs.9 or 11. At critical condition the value of a is taken to be a_c in Eqs.7 and 8. The integration of the Eq.8 is done by using Gauss-Chebyshev quadrature method because of existence of singularity at the integral boundary.

As shown in Fig.2, two conditions at critical load, i.e., $CTOD_c \le w_s$ and $w_s \le CTOD_c \le w_c$ may arise at the notch-tip while using bilinear softening function. For specimens subjected to temperatures less than 120ºC, the critical $CTOD_c$ is less than w_s; whereas, for temperatures higher than 120ºC, the critical $CTOD_c$ is wider than w_s.

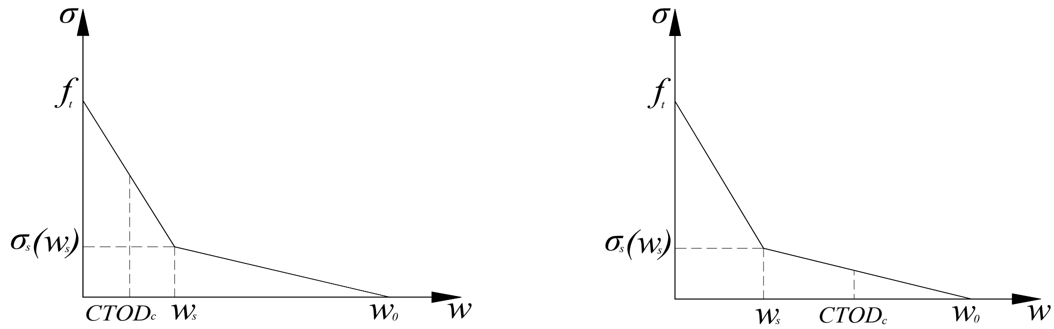

(a) When $CTOD_c \le w_s$ (b) When $CTOD_c > w_s$

Fig.2. Two different situations for $CTOD_c$ and w_s

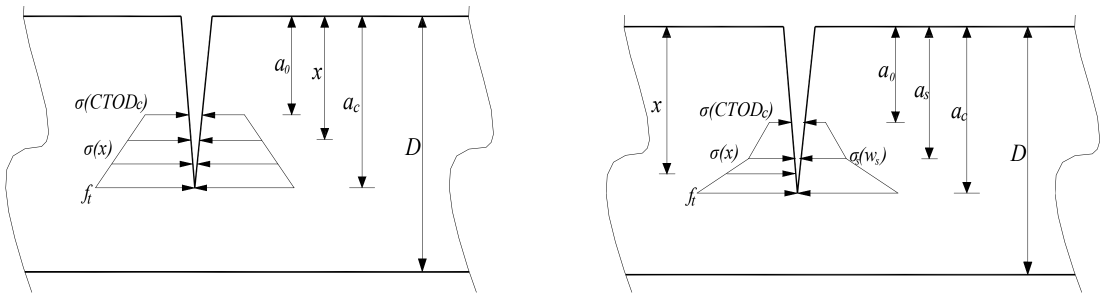

(a) The linear distribution of cohesive force (b) The bilinear distribution of cohesive force

Fig.3. Cohesive force distribution along the crack length at critical load

A. When the critical $CTOD_c$ corresponding to maximum load P_u is less than w_s as shown Fig.2a. The distribution of cohesive stress along the fictitious fracture zone is approximated to be linear as shown in Fig.3a. The variation of cohesive stress along the fictitious fracture zone for this loading condition i.e., $a_o \le a \le a_c$ or $0 \le CTOD \le CTOD_c$ is written as:

$$\sigma(x)=\sigma(CTOD_c)+(f_t-\sigma(CTOD_c))(x-a_0)/(a_c-a_0) \tag{9}$$

where, σ ($CTOD_c$) is the critical values of cohesive stress being at the tip of initial notch. The value of σ ($CTOD_c$) is determined by using bilinear softening function:

$$\sigma(CTOD_c)=\sigma_s(w_s)+\frac{w_s-CTOD_c}{w_s}(f_t-\sigma_s(w_s)) \tag{10}$$

B. When the critical $CTOD_c$ corresponding to maximum load P_u is wider than w_s as shown Fig.2b. The distribution of cohesive stress along the fictitious fracture zone is approximated to be bilinear as shown in Fig.3b. The variation of cohesive stress along the fictitious fracture zone for this loading condition, also, $a_o \le a \le a_c$ or $0 \le CTOD \le CTOD_c$ is written as:

$$\begin{cases} \sigma_1(x) = \sigma(CTOD_c) + (\sigma_s(w_s) - \sigma(w))\dfrac{(x - a_0)}{(a_s - a_0)} & a_s \le x \le a_0 \\ \sigma_2(x) = \sigma_s(w_s) + (f_t - \sigma_s(w_s))\dfrac{(x - a_s)}{(a_c - a_s)} & a_s \le x \le a_c \end{cases} \tag{11}$$

The value of σ ($CTOD_c$) is determined by using bilinear softening function:

$$\sigma(CTOD_c) = \frac{w_0 - CTOD_c}{w_0 - w_s}\sigma_s(w_s) \tag{12}$$

The limits of integration of Eq.7 should be taken in two steps: $a_o \le x \le a_s$ for cohesive stress $\sigma_1(x)$ and $a_s \le x \le a_c$ for cohesive stress $\sigma_2(x)$ respectively. The same Green's function F(x/a, a/h) for a given effective crack extension will be determined using Eq.8. The calculated formula is listed as follows:

$$K_I{}^{c} = \int_{a_0}^{a_s} 2\sigma_1(x)F(\frac{x}{a_c},\frac{a_c}{h})/\sqrt{\pi a_c}\,dx + \int_{a_s}^{a_c} 2\sigma_2(x)F(\frac{x}{a_c},\frac{a_c}{h})/\sqrt{\pi a_c}\,dx \tag{13}$$

The effective crack length at break point a_s (shown in Fig.3b), is computed from the following nonlinear expression [24] by substituting COD (a_s), $CMOD$, a_c and h:

$$COD(a_s) = CMOD\{(1 - \frac{a_s}{a_c})^2 + (1.018 - 1.149\frac{a_c}{h})[\frac{a_s}{a_c} - (\frac{a_s}{a_c})^2]\}^{1/2} \tag{14}$$

Where COD (a_s) is the crack opening displacement at a_s, a_c is the effective crack length (according to Eq.4) and h is the specimen height.

4. Proposed method to determine cohesive fracture toughness using weight function

4.1. Introduction of weight function

Use of weight functions for calculation of stress intensity factors provides an efficient analytical technique for fracture mechanics applications. The method of weight function was initially proposed by Bueckner [28] and Rice [29] for determination of stress intensity factors and crack face displacements in cracked bodies under arbitrary applied stress fields. The value of cohesive fracture toughness K_s may be directly determined using weight function as below:

$$K_S = \int_0^a \sigma_s(x)m(x,a)dx_s \tag{15}$$

The term $m(x, a)$ in Eq.15 is known as weight function and expressed as:

$$m(x,a) = \frac{E'}{2K_r}\frac{\partial u_r}{\partial a} \tag{16}$$

where, a = crack length; $\sigma_s(x)$ = the stress distribution along the crack line in the uncracked body under the loading case s, which can be determined either experimentally or numerically or analytically; dx_s= the infinitesimal length along the crack surface; $E'= E$ for plane stress and $E'= E/1-\nu^2$ for plane strain, E and ν are the Young's modulus and the Poisson's ratio respectively.

4.2. Determination of universal weight function for an edge crack in finite width plate

Several one-dimensional weight functions with various mathematical forms are available in literature [31-33] but their use is limited. Glinka and Shen [34] introduced one universal form of weight function expression having four terms, which can be used for variety of one-dimensional Mode I crack problems:

$$m(x,a) = \frac{2}{\sqrt{2\pi(a-x)}}[1 + M_1(1-\frac{x}{a})^{1/2} + M_2(1-\frac{x}{a}) + M_3(1-\frac{x}{a})^{3/2}] \tag{17}$$

For i=1，3 $M_i = \frac{1}{\sqrt{(1-a/D)^3}}[a_i + b_i a/D + c_i(a/D)^2 + d_i(a/D)^3 + e_i(a/D)^4 + f_i(a/D)^5]$ (18)

For i=2 $M_i = [a_i + b_i a/D]$ (19)

The values of coefficients a_i, bi, c_i, d_i, e_i, f_i are given in Table 1. For an edge crack in the finite width of plate the accuracy of the weight function are verified with respect to Tada et al. [27] Green's function.

Table 1 Coefficients of four terms weight function parameters M_1, M_2 and M_3

i	a_i	b_i	c_i	d_i	e_i	f_i
1	0.0572	-0.8742	4.0466	-7.8994	7.8550	-3.1883
2	0.4935	4.4365				
3	0.3404	-3.9534	16.1904	-16.0959	14.6302	-6.1307

4.3. Evaluation of cohesive fracture toughness

Once the weight function parameters are determined, Eq.15 is used to calculate the stress intensity factor at critical condition due to cohesive stress distribution as shown in Fig.3. The value of $\sigma(x)$ in Eq.15 is replaced by Eq.10, Eq.11, hence the closed form expression of K_I^c is can be obtained. The value of K_I^c using four terms weight function is expressed in the following form.

A. When the critical $CTOD_c$ corresponding to maximum load P_u is less than w_s as shown Fig.2a:

$$K_I^{\ c} = \int_0^{a_c} \{\sigma(CTOD_c) + (f_t - \sigma(CTOD_c))(x-a_0)/(a_c-a_0)\} \times \frac{2}{\sqrt{2\pi(a_c-x)}}[1 + M_1(1-\frac{x}{a_c})^{1/2} + M_2(1-\frac{x}{a_c}) + M_3(1-\frac{x}{a_c})^{3/2}]dx_s \tag{20}$$

After integration of Eq.20 the closed form solution of K_I^c is determined as:

$$K_{Ic} = \frac{2}{\sqrt{2\pi a_c}}(A_1 B_1 a_c + A_2 B_2 a_c^{\ 2}) \tag{21}$$

Where $A_1 = \sigma(CTOD_c)$, $A_2 = \frac{f_t - \sigma(CTOD_c)}{a_c - a_0}$, $S = (1 - a_0/a_c)$,

$B_1 = 2S^{1/2} + M_1 S + 2/3 M_2 S^{3/2} + M_3 S^2/2$, $B_2 = 4/3 S^{3/2} + M_1 S^2/2 + 4/15 M_2 S^{5/2} + M_3 S^3/6$.

B. When the critical $CTOD_c$ corresponding to maximum load P_u is wider than w_s as shown Fig.2b.

$$K_I^{\ c} = \int_0^{a_c} \left\{\sigma(CTOD_c) + (\sigma_s(w_s) - \sigma(w))\frac{(x-a_0)}{(a_s-a_0)} + \sigma_s(w_s) + (f_t - \sigma_s(w_s))\frac{(x-a_s)}{(a_c-a_s)}\right\} \times \frac{2}{\sqrt{2\pi(a_c-x)}}[1 + M_1(1-\frac{x}{a_c})^{1/2} + M_2(1-\frac{x}{a_c}) + M_3(1-\frac{x}{a_c})^{3/2}]dx_s \tag{22}$$

After integration of Eq.22 the closed form solution of K_I^c is determined as:

$$K_I^{\ c} = \frac{2}{\sqrt{2\pi a_c}}\{A_1 a_c [B_1 - B_3] + A_3 a_c^{\ 2}[B_1 - B_3 - B_4 + B_5]\} - \frac{2}{\sqrt{2\pi a_c}}\{A_3 a_c a_0 [B_1 - B_3]\} + \frac{2}{\sqrt{2\pi a_c}}\{A_4 B_3 a_c + A_5 B_3 a_c^{\ 2}\} - \frac{2}{\sqrt{2\pi a_c}}\{A_5 a_c a_s B_3\} + \frac{2}{\sqrt{2\pi a_c}}\{A_5 B_5 a_c^{\ 2}\} \tag{23}$$

Where $A_1=\sigma(CTOD_c)$, $A_3=\dfrac{\sigma_s(w_s)-\sigma(CTOD_c)}{a_c-a_0}$, $A_4=\sigma_s(w_s)$, $A_5=\dfrac{f_t-\sigma_s(w_s)}{a_c-a_0}$,

$B_1=2S_1^{1/2}+M_1S_1+2/3M_2S_1^{3/2}+M_3S_1^2/2$, $B_3=2S_2^{1/2}+M_1S_2+2/3M_2S_2^{3/2}+M_3S_2^2/2$,

$B_4=2/3S_1^{1/2}+M_1S_1^2/2+2/5M_2S_1^{5/2}+M_3S_1^3/3$, $B_5=2/3S_2^{3/2}+M_1S_2^2/2+2/5M_2S_2^{5/2}+M_3S_2^3/3$,

$S_1=(1-a_0/a_c)$, $s_2=(1-a_s/a_c)$.

5 Calculation of double-K fracture parameters

The two parameters (K_I^{ini} and K_I^{un}) of double-K fracture criterion for wedge-splitting test is determined using linear elastic fracture mechanics formula given in XU[8]:

$$K(P,a)=\frac{P\times 10^{-3}}{th^{1/2}}f(\alpha) \tag{24}$$

$$f(\alpha)=\frac{3.675\times[1-0.12(\alpha-0.45)]}{(1-\alpha)^{3/2}},\alpha=\frac{a}{h} \tag{25}$$

The empirical expression (24) is valid within 2% accuracy for, $0.2\le\alpha\le 0.8$.

Equations 24 and 25 can be used in calculation of unstable fracture toughness, K_I^{un} at the tip of effective crack length a_c, in which a = a_c and P = maximum load, P_u for TPBT and CT test specimen geometries respectively. The initiation toughness, K_I^{ini} is calculated using Eqs.24 and 25 when the initial cracking load, P_{ini} at initial crack tip is known. In present paper, the P_{ini} is determined by graphical method using the starting point of non-linearity in *P-CMOD* curve described in the following section.

Generally, for post-fire concrete specimens the value of initial fracture toughness K_I^{ini} is far less than the value of critical fracture toughness K_I^{un}, especially for higher temperatures. So much more consideration is put to the critical fracture toughness K_I^{un}. In double-K fracture model, the following relation can be employed:

$$K_I^{un}=K_I^{ini}+K_I^{c} \tag{26}$$

Since there are two methods to determine the cohesive fracture toughness as mentioned above. Here we donate the experimental value, analytical value and weight function value of critical fracture toughness as $K_I^{un\text{-}e}$, $K_I^{un\text{-}A}$, $K_I^{un\text{-}W}$ respectively, and from which we would judge the validation of double-K fracture model and weight function method to the post-fire concrete.

6. Experimental validation and comparison of results

6.1. Experimental program and experimental phenomena

To obtain the complete *P-CMOD* curves, the wedge-splitting tests were implemented. A total of 50 concrete specimens with the same dimensions 230×200×200 mm were prepared, the geometry of the specimens is shown in Fig.4 (b=200mm, d=65mm, h=200mm, f=30mm, a_0=80mm, θ=15°). The concrete mix ratios (by weight) were Cement: Sand: Coarse aggregate: Water = 1.00:3.44:4.39:0.80, with common Portland cement-mixed medium sand and 16-mm graded coarse aggregate. All the specimens had a precast notch of 80 mm height and 3 mm thickness, achieved by placing a piece of steel plate into the molds prior to casting. Each wedge splitting specimen was embedded with a thermal couple in the center of specimen for temperature control.

Nine heating temperatures, ranging from 65ºC to 600ºC (T_m=65ºC, 120ºC, 200ºC, 300ºC, 350ºC, 400ºC, 450ºC, 500ºC, 600ºC), were adopted with the ambient temperature as a reference. Because it was recognized that the fracture behavior measurements were generally associated with significant scatter, five repetitions were performed for each temperature.

A closed-loop servo controlled hydraulic jack with a maximum capacity of 1000 kN was employed to conduct the wedge splitting tests (shown in Fig.5). Two Clip-on Extensometers were suited at the mouth and the tip of the crack to measure the crack mouth opening displacement (*CMOD*) and crack tip opening displacement (*CTOD*). To obtain the complete *P-CMOD* curves (shown in Fig.6), the test rate was fixed at 0.4 mm/min.

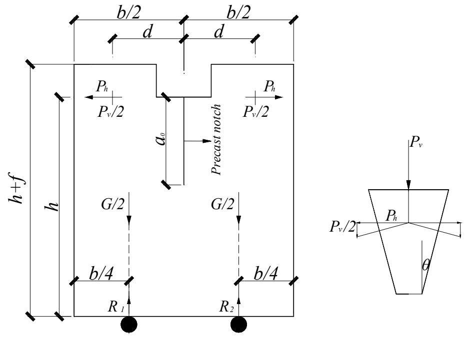

Fig. 4. The geometry of specimens

Fig. 5. The experiment set-up

For the specimens exposed to relatively lower temperatures (20ºC~200ºC), the splitting load generally reached its peak with no visible crack observed. Once the first crack initiated, the splitting load dropped dramatically. For temperatures at 20ºC~200ºC shows that the crack propagated vertically to the bottom of the specimen along with the precast notch. At temperatures above 200ºC, more than one crack branched from the tip of notch, competing to form the final fracture (shown in Fig.7).

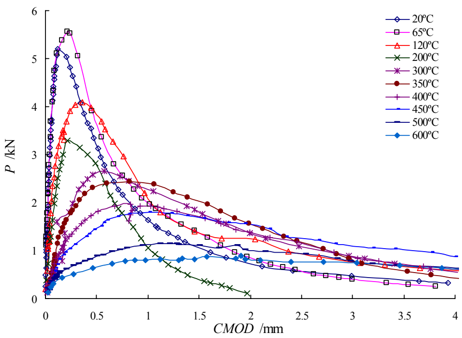

Fig.6.*P* vs *CMOD* curves of specimens with temperatures

Fig. 7. Testing phenomenon of post-fire specimens

6.2. Experimental results

Fig.6 shows typical complete load-displacement curves for different heating temperatures up to 600ºC. The figure shows that the ultimate load P_u decreases significantly with increasing temperatures T_m, whereas the crack-mouth opening displacement (*CMOD*) increases with T_m. The initial slope of ascending branches decrease with heating temperatures, and the curves become gradually shorter and more extended.

The recorded maximum load P_u, the recorded crack mouth opening displacement $CMOD_c$ at P_u, the calculated crack tip opening displacement $CTOD_c$ based on Eq.14, the initial cracking load P_{ini} determined by graphical method, the calculated residual Young's modulus E based on Eq.5, the double-K fracture parameters, i.e., K_I^{ini} and $K_I^{un\text{-}E}$ and the residual fracture energy G_F are summarized in Table 2. Here we only list part of the statistics.

Table 2 The experimental results of fracture parameters

speci men	tempe rature	P_{ini}/ kN	P_{max}/ kN	$CMOD_c$ /mm	$CTOD_c$ /mm	E GPa	G_F N/m	K_I^{ini} MPa·m$^{1/2}$	$K_I^{c\text{-}A}$ MPa·m$^{1/2}$	$K_I^{c\text{-}W}$ MPa·m$^{1/2}$	$K_I^{un\text{-}E}$ MPa·m$^{1/2}$	$K_I^{un\text{-}A}$ MPa·m$^{1/2}$	$K_I^{un\text{-}W}$ MPa·m$^{1/2}$
WS1		6.19	8.33	0.174	0.065	15.30	234.15	0.505	0.666	0.691	1.061	1.171	1.196
WS2		6.28	9.81	0.120	0.039	20.51	483.66	0.523	0.571	0.608	1.070	1.094	1.131
WS3	20ºC	7.26	10.40	0.210	0.079	20.66	438.22	0.610	0.968	1.002	1.497	1.578	1.612
WS4		7.02	7.92	0.152	0.060	18.88	219.39	0.357	0.799	0.818	1.091	1.156	1.175
WS5		5.65	9.39	0.237	0.096	15.45	321.05	0.503	0.715	0.742	1.213	1.218	1.245
Aver		6.55	9.17	0.178	0.068	18.16	339.30	0.498	0.744	0.772	1.186	1.243	1.271
WS11		5.03	8.37	0.191	0.056	10.65	396.52	0.518	0.45	0.489	0.900	0.968	1.007
WS13		4.69	8.25	0.224	0.084	11.87	517.82	0.417	0.745	0.754	1.058	1.162	1.171
WS12	120ºC	4.71	7.53	0.357	0.152	9.48	654.73	0.419	1.016	1.070	1.202	1.435	1.489
WS14		2.79	7.53	0.198	0.083	15.42	345.46	0.249	0.858	0.951	1.107	1.107	1.200
WS15		——	——	——	——	——	——	——	——	——	——	——	——
Aver		4.31	7.92	0.243	0.094	9.48	478.63	0.401	0.767	0.816	1.067	1.168	1.217
WS21		1.89	3.40	0.653	0.283	2.45	437.92	0.168	0.45	0.478	0.556	0.618	0.646
WS22		3.48	5.53	0.667	0.280	3.49	611.47	0.309	0.553	0.597	0.841	0.862	0.906
WS23	300ºC	1.82	3.38	0.672	0.271	1.91	341.77	0.162	0.374	0.386	0.480	0.536	0.548
WS24		2.61	4.97	0.577	0.262	1.99	564.12	0.232	0.359	0.381	0.589	0.591	0.613
WS25		2.03	4.17	0.651	0.361	4.03	549.99	0.175	0.82	0.824	0.913	0.995	0.999
Aver		2.37	4.29	0.644	0.291	2.78	501.05	0.209	0.512	0.533	0.676	0.21	0.742
Aver		2.01	3.78	0.901	0.410	1.56	490.71	0.149	0.374	0.398	0.615	0.526	0.550
WS36		1.52	3.37	1.009	0.544	1.41	611.53	0.135	0.387	0.401	0.582	0.522	0.536
WS37		——	——	——	——	——	——	——	——	——	——	——	——
WS38	450ºC	1.52	3.26	1.419	0.660	1.46	482.45	0.135	0.341	0.375	0.527	0.476	0.510
WS39		1.12	3.07	1.348	0.617	1.34	663.10	0.100	0.42	0.437	0.563	0.520	0.537
WS40		0.99	2.94	1.394	0.666	1.58	678.79	0.088	0.513	0.508	0.659	0.601	0.596
Aver		1.29	3.16	1.293	0.622	1.16	608.97	0.115	0.415	0.430	0.583	0.530	0.545
WS46		0.76	1.13	1.482	0.684	0.47	228.23	0.067	0.174	0.188	0.221	0.231	0.245
WS47		0.53	1.48	2.082	0.684	0.48	395.06	0.063	0.209	0.216	0.277	0.284	0.291
WS48	600ºC	0.81	1.65	1.908	0.813	1.14	539.22	0.072	0.478	0.512	0.550	0.550	0.584
WS49		0.58	1.14	1.687	0.973	0.38	331.99	0.052	0.188	0.198	0.225	0.225	0.235
WS50		0.62	1.48	2.082	0.727	0.38	273.07	0.068	0.155	0.161	0.213	0.213	0.219
Aver		0.62	1.38	1.848	0.799	0.57	353.51	0.064	0.241	0.255	0.297	0.301	0.315

6.3. Discussion

In order to express the influence on the residual fracture toughness in detail, Fig.8 plots the tendency of initial fracture toughness K_I^{ini} and the unstable fracture toughness K_I^{un} with heating temperatures T_m. It is concluded that the two fractures toughness decrease monotonously with T_m because of the thermal damage induced by the heating temperatures.

The initial fracture toughness continuously decreases from 0.498 kN at room temperature to 0.269 kN at 200ºC, 0.115 kN at 450ºC, and finally 0.064kN at 600ºC, with a significant loss of 0.434 kN or 96%. The unstable fracture toughness decreases from 1.186 kN at room temperature to 0.297 at 600ºC, with a significant loss of 0.889 kN or 75%.

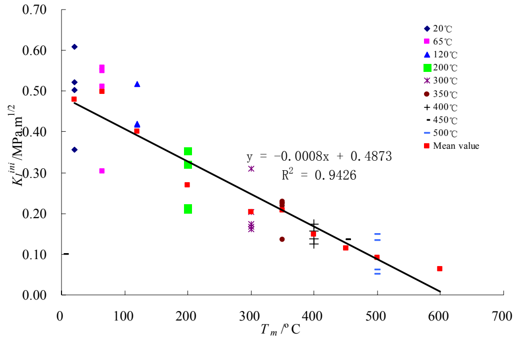

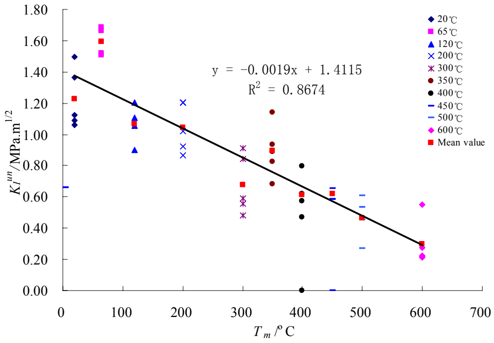

(a) The tendency of K_I^{ini} with T_m (b) The tendency of K_I^{un} with T_m

Fig.8. The tendency of residual fracture toughness with heating temperatures T_m

Comparing the result shown in Table 2, it can be known that the value of $K_I^{un\text{-}A}$ evaluated by formula (26) has a good coincidence to one calculated by inserting the values of P_{max} and a_c=D into the formula (24), i.e. the critical fracture toughness from analytical and experimental method. Fig.9 shows the relationship between the two parameters. The similar results could be concluded between the value of $K_I^{un\text{-}W}$ from formula (26) and the experimental results from formula(24).

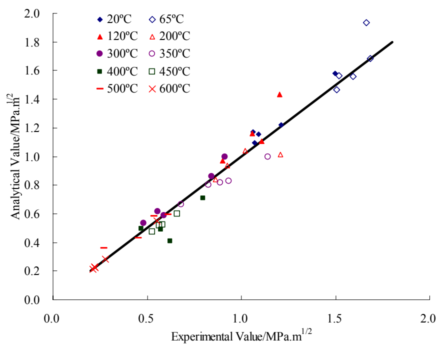

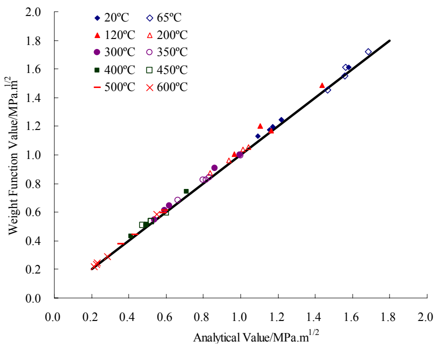

Fig.9. Comparison between analytical and experimental values of critical fracture toughness

Fig.10. Comparison between analytical and weight function values of critical fracture toughness

In totally 45 effective specimens, the deviation between $K_I^{un\text{-}A}$ and $K_I^{un\text{-}E}$ of 22 specimens is below 5%, and of 40 specimens is below 15%, account for 89%of total specimens. Accordingly, the number of specimens corresponding to the same deviation between $K_I^{un\text{-}W}$ and $K_I^{un\text{-}E}$ is 20 and 42, respectively.

Fig.10shows the weight function method agrees well with the analytical method, and the deviation below 5% accounts for 65% of total specimens.

7. Conclusion

The determination of double-K fracture parameter using both analytical and weight function methods are carried out in present research. In calculating the cohesive fracture toughness, two conditions are divided at critical load: for specimens subjected to temperatures less than 120ºC, the critical $CTOD_c$ is less than w_s; whereas, for temperatures higher than 120ºC, the critical $CTOD_c$ corresponding to maximum load P_u is wider than w_s. This part of work would be a useful supplement to the existed analysis.

Wedge-splitting tests with ten temperatures varying from 20ºC to 600ºC are implemented. The complete load-crack opening displacement curves are obtained and the initial and critical fracture toughness could be calculated experimentally.

The validation of double-K fracture model to the post-fire concrete specimens is proved. In totally 45 effective specimens, the deviation between analytical value $K_I^{un\text{-}A}$ and experimental $K_I^{un\text{-}E}$ of 22 specimens is below 5%, and of 40 specimens is below 15%, account for 89% of total specimens. Accordingly, the number of specimens corresponding to the same deviation between $K_I^{un\text{-}W}$ and $K_I^{un\text{-}E}$ is 20 and 42, respectively. Meanwhile the weight function method agrees well with the analytical method, and the deviation below 5% accounts for 65% of total specimens.

Acknowledgment

The State Laboratory of Disaster Reduction in Civil Engineering (SLDRCE09-D-02) has supported this research.

.

Reference

[1] HILLERBORG A., MODEER M. and PETERSON P.E. Analysis of crack formation and crack growth in concrete by means of fracture mechanics and finite elements. Cem Concr Res, 6(6), (1976) 773-782.
[2] Bazant ZP, Oh BH. Crack band theory for fracture of concrete. Mater Struct, 16(93) (1983) 155-177.
[3] Jenq YS, Shah SP Two parameter fracture model for concrete. J Engng Mech, ASCE, 111(10) (1985) 1227-1241.
[4] Nallathambi P, Karihaloo BL. Determination of specimen-size independent fracture toughness of plain concrete. Mag Concr Res, 38(135) (1986) 67-76.
[5] Bazant ZP, Kazemi MT. Determination of fracture energy, process zone length and brittleness number from size effect, with application to rock and concrete. Int J Fract, 44 (1990) 111-131.
[6] Xu S, Reinhardt HW. Determination of double-K criterion for crack propagation in quasi-brittle materials, Part I: Experimental investigation of crack propagation. Int J Fract, 98 (1999) 111-149.
[7] Xu S, Reinhardt HW. Determination of double-K criterion for crack propagation in quasi-brittle materials, Part II: Analytical evaluating and practical measuring methods for three-point bending notched beams. Int J Fract, 98 (1999)151-177.
[8] Xu S, Reinhardt HW. Determination of double-K criterion for crack propagation in quasi-brittle materials, Part III: Compact tension specimens and wedge splitting specimens. Int J Fract, 98 (1999) 179-193.
[9] Jenq YS, Shah SP. A fracture toughness criterion for concrete. Engng Fract Mech, 21(5) (1985) 1055-1069.
[10] Kumar S, Barai SV. Determining the double-K fracture parameters for three-point bending notched concrete beams using weight function. Fatigue Fract Engng Mater Struct, 33(2010) 645-660.
[11] Murakami. Stress Intensity factors handbook. London: Pergamon Press, 1987.
[12] Shailendra Kumar, S. V. Barai. Influence of specimen geometry and size-effect on the KR-curve based on the cohesive stress in concrete. Inter J Fract, 152 (2008) 127-148.
[13] Shailendra Kumar, S. V. Barai. Influence of specimen geometry on determination of double-K fracture parameters of concrete: a comparative study. Inter J Fract, 149 (2008) 47-66.
[14] Karihaloo B L, Nallathambi P. Size effect prediction from the double-K fracture model for notched concrete. Materials and structures, 1990, 23: 178-185.
[15] Zdenek. P. Bazant and Pere C. Prat: Effect of Temperatures and Humidity on Fracture Energy of Concrete. ACI Mater J, 85(4) (1988) 262-271.

[16] Baker G: The effect of exposure to elevated temperatures on the fracture energy of plain concrete. RILEM Mater Struc, 29 (190)(1996) 383-388.
[17] Zhang B., Bicanic N., Pearce C.J. and Balabanic G.: Residual fracture properties of normal and high-strength concrete subject to elevated temperatures. Mag Concr Res, 52(2) (2000) 123-136.
[18] Nielsen C.V. and Bicanic N.: Residual fracture energy of high-performance and normal concrete subject to high temperatures. RILEM Mater Struc, 36 (262) (2003) 515-521.
[19] B. Zhang and N. Bicanic: Fracture energy of high-performance concrete at high temperatures up to 450ºC: the effects of heating temperatures and testing conditions (hot and cold). Mag Concr Res 58 (5) (2006) 277-288.
[20] G.Prokopski: Fracture toughness of concretes at high temperature. J Mater Sci, 30(1995) 1609-1612.
[21] Hisham Abdel-Fattah and Sameer A.Hamoush: Variation of the fracture toughness of concrete with temperature. Constr Build Mater, 11(2) (1997) 105-108.
[22] Petersson PE. Crack growth and development of fracture zones in plain concrete and similar materials. Division of Building Materials, Lund Institute of Technology, Report TVBM-1006, Sweden, 1981.
[23] Gopalaratnam VS, Shah SP. Softening response of plain concrete in direct tension. ACI J May-June (1985) 310-323.
[24] Reinhardt HW, Cornelissen HAW, Hordijk DA. Tensile tests and failure analysis of concrete. J Struc Engng ASCE, 112 (1986) 2462-2477.
[25] Hilsdorf HK, Brameshuber W. Code-type formulation of fracture mechanics concepts for concrete. Inter J Fract, 51 (1991) 61-72.
[26] Phillips DV, Zhang Z. Direct tension tests on notched and un-notched plain concrete specimens. Mag Concr Res, 45 (1993) 25-35.
[27] Tada H, Paris PC, Irwin G. The stress analysis of cracks handbook. Paris Productions Incorporated, St. Louis, 1985.
[27] Bueckner HF. A novel principle for the computation of stress intensity factors. Z Angew Math Mech, 50(1970) 529-546.
[28] Rice JR. Some remarks on elastic crack-tip stress fields. Int J Solid Struct, 8 (1972) 751-758
[29] Shailendra Kumar, S. V. Barai. Determining double-K fracture parameters of concrete for compact tension and wedge splitting tests using weight function. Engng Fract Mech, 76(7) (2009) 935-946.
[30] Fett T. Limitations of the Petroski－Achenbach procedure demonstrated for a simple load case. Engng Fract Mech, 29(6) (1988) 713-716.
[31] Fett T, Mattheck C, Munz D. On calculation of crack opening displacement from the stress intensity factor. Engng Fract Mech 27 (1987) 697-715.
[32] Glinka G, Shen G. Universal features of weight functions for cracks in Mode I. Engng Fract Mech, 40(6) (1991) 1135-1146.